

A Dynamical Systems Approach to Modeling and Analysis of Transactive Energy Coordination

Md Salman Nazir, *Member, IEEE*, and Ian A. Hiskens, *Fellow, IEEE*

Abstract—Under transactive (market-based) coordination, a population of distributed energy resources (DERs), such as thermostatically controlled loads (TCLs) and storage devices, bid into an energy market. Consequently, a certain level of demand will be cleared based on the operating conditions of the grid. This paper analyzes the influence of various factors, such as price signals, feeder limits, and user-defined bid functions and preferences, on the aggregate energy usage of DERs. We identify cases that can lead to load synchronization, undesirable power oscillations and highly volatile prices. To address these issues, the paper develops an aggregate model of DERs under transactive coordination. A set of Markov transition equations have been developed over discrete ranges (referred to as “bins”) of price levels and their associated DER operating states. A detailed investigation of the performance of this aggregate model is presented. With reformulation of the transition equations, the bin model has been incorporated into a model predictive control setting using both mixed integer programming and quadratic programming. A case study shows that a population of TCLs can be managed economically while avoiding congestion in a distribution grid. Simulations also demonstrate that power oscillations arising from synchronization of TCLs can be effectively avoided.

Index Terms—Transactive coordination; Distribution markets; Load synchronization; Thermostatically controlled loads; Distributed energy resources; Model predictive control.

I. INTRODUCTION

Transactive energy coordination mechanisms have been proposed as a framework for managing large numbers of distributed energy resources (DERs), such as thermostatically controlled loads (TCLs), energy storage and electric vehicles, in an electric grid [1]–[3]. Such schemes provide users with the flexibility to consume energy based on the price they are willing to pay. Several recent studies and demonstration projects have shown the applicability of such mechanisms to manage the aggregate demand of residential electric loads and commercial building heating, ventilation, and air conditioning (HVAC) systems [1]–[6]. Applications include reduction of peak demand, provision of regulation services and congestion relief.

Under transactive (market-based) energy coordination, a population of distributed resources bids into the energy market and a certain level of demand is cleared, depending on the operating conditions of the grid. This process is primarily based on a double auction mechanism [2]. A market mechanism proposed in [3] can attain economically efficient

market outcomes while taking into account individual device dynamics. The applicability of this approach and the influence of different system parameters have been studied in [4]. While these market-based schemes can attain economically efficient outcomes, concerns remain regarding the impact on system stability. Previous analyses of electricity market dynamics [7], [8] have highlighted the possibility of power oscillations and highly volatile prices. Our recent work [9] applied the bidding strategy described in [2] (also in Section II of [3]) to show undesirable oscillatory response of a population of air-conditioners. Simulations suggest that several factors may contribute to load synchronization and power oscillations, including prolonged flat price signals followed by sharp changes in the price, feeder limits that are set too low and that are encountered periodically, and the form of user bid curves. A detailed analysis of emergent oscillations was beyond the scope of [9] and will be elaborated upon in this paper.

It has been shown in [10] and [11] that oscillations may appear under market-based coordination of DERs. In [10], oscillatory behavior was observed in the aggregate demand when simulating a large number of price-responsive electric vehicles. It was shown in [11] that while oscillations may be present, the aggregate demand from a population of DERs can reach the stable equilibrium provided the user-defined bid slopes are not too steep. This work considered a generalized aggregate battery model. Our proposed framework also builds upon a generalized battery model. Additionally, we introduce the concept of *lockout conditions* to account for customers who desire periods of uninterrupted supply. The possibility and nature of oscillations in the aggregate demand, given the presence of such lockout conditions, will be studied.

Prior analysis has clearly demonstrated that the aggregate demand of DERs can be affected by price signals, feeder capacity limits, and DER bidding strategies. However, predicting the aggregate behavior of DERs under transactive energy coordination and guaranteeing stability remains a challenging task [9], [11]. Therefore, this paper focuses largely on developing an aggregate model of DERs under market-based coordination. To accomplish this goal, a set of Markov transition equations are developed over discrete ranges of DER energy and price levels (here referred to as “bins”). Lockout conditions are also incorporated. Eigenvalues of the resulting system matrix provide insights into system behavior. Although bin-based aggregate models have been used extensively for controlling aggregations of TCLs [12]–[15], application to the transactive coordination framework has not previously been considered. Hence, a novel contribution of this paper is the extension of the bin-modeling approach to market-based coordination schemes for DERs. Furthermore, incorporating this model in a model

Authors are with the Department of Electrical Engineering and Computer Science, University of Michigan, Ann Arbor, MI, USA. Emails: mdsnazir@umich.edu, hiskens@umich.edu.

The authors gratefully acknowledge the contribution of the Natural Sciences and Engineering Research Council of Canada (NSERC) and the U.S. National Science Foundation through grant CNS-1238962.

predictive control (MPC) framework allows the calculation of optimal price signals for achieving desired DER energy usage. A reformulation of the transition equations ensures that the modified model remains linear for optimization-based market clearing strategies. However, a set of logical constraints are needed to model the market clearing behavior. Thus, a mixed integer formulation is obtained, providing a further contribution to aggregate modeling and market-based coordination of DERs. Additionally, relaxation of the integer model results in a quadratic program that is computationally more efficient. Measures to avoid synchronization are also incorporated in the MPC strategy.

Finally, we consider an application of MPC to manage a population of DERs in a distribution system. Several recent studies have shown that with increased penetration of controllable loads and storage devices, advanced congestion management techniques will be necessary to avoid simultaneous consumption from DERs and to limit payback from unsatisfied demand [16]–[20]. Hence, we show that a population of TCLs can be managed economically while avoiding congestion in a distribution grid. Simulations also demonstrate that synchronization of TCLs and undesired power oscillations can be effectively avoided. The MPC formulation considers system level costs, operational constraints and constraints related to the DER population. Consequently, the generated price signals induce desirable behavior of the DER population. This addresses an important gap in transactive coordination as previous studies [1]–[4] have taken price signals to be exogenous inputs rather than generated via feedback.

The remainder of the paper is organized as follows. Section II describes the modeling background, and presents analysis of the behavior of DERs under transactive coordination. Section III presents the bin-based aggregate model for DERs under market-based coordination. Section IV presents the model predictive control (MPC) framework for controlling the DERs. Both a mixed-integer formulation and a relaxed quadratic program formulation are considered. Section V provides simulation results showing the performance of the aggregate model and the MPC controller. Section VI concludes by summarizing our findings and discussing their implications.

II. PROBLEM FORMULATION AND ANALYSIS

A. Single DER Dynamic Model

The state dynamics of DERs, such as TCLs, electric vehicles and batteries, can be expressed using a generalized battery model [21], [22]. Let $e_{j,k}$ be the j -th DER's energy state, i.e. its state of charge (SOC), at time k . Then, the evolution in $e_{j,k}$ can be modeled with the discrete-time difference equation,

$$e_{j,k+1} = a_j e_{j,k} + d_{j,k}, \quad (1)$$

where $e_j^{\min} \leq e_{j,k} \leq e_j^{\max}$, and $d_{j,k}$ is the power consumed, with $d_j^{\min} \leq d_{j,k} \leq d_j^{\max}$. The coefficient a_j is the j -th DER's energy dissipation rate, with $a_j \in (0, 1]$ for TCLs and HVAC systems, and $a_j \approx 1$ for storage devices [11]. Assume $e_{j,k}$ is normalized, i.e. $e_j^{\min} = 0$ and $e_j^{\max} = 1$. Considering $u_{j,k} \in \{0, 1\}$ is the

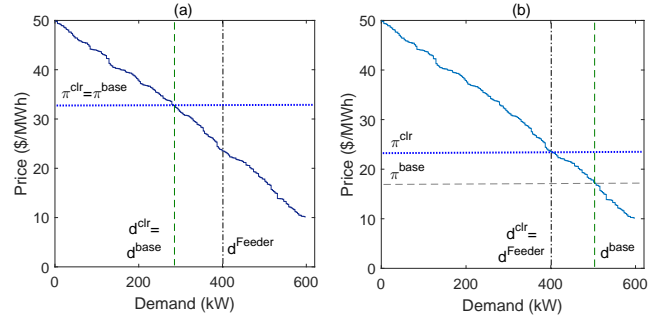


Fig. 1. (a) Market clearing with feeder capacity not exceeded. (b) Market clearing with feeder capacity exceeded [2], [9].

discrete power on/off decision, and γ_j is the charging efficiency (i.e. the energy gain if the DER is on), we can write,

$$e_{j,k+1} = a_j e_{j,k} + \gamma_j u_{j,k}. \quad (2)$$

The specifics on temperature dynamics of TCLs, along with example parameter values, are provided in Appendix VII-A.

Next, let $\pi_{j,k}$ be the j -th DER's bid price at time k . Typically $\pi_{j,k}$ decreases as $e_{j,k}$ increases. Therefore, the bid function relating $\pi_{j,k}$ and $e_{j,k}$ can be expressed as,

$$\pi_{j,k} = \pi_j^{\max} - \beta_j e_{j,k}, \quad (3)$$

where π_j^{\max} is the bid price when $e_{j,k} = 0$ and β_j represents the slope of the bid curve.

B. Market Clearing Mechanism

Several different market-based coordination mechanisms have been proposed in the literature [2], [3], [23]. For analysis purposes, we primarily focus on the mechanism proposed in [2] (also given in Section II of [3]) and suggest generalizations in later sections. To summarize, the DERs are assumed to be connected to a distribution feeder, which clears an allowable demand level at a particular price. Let π_k^{base} be the base price forecast at the k -th time period. An aggregator gathers anonymous bids (price versus demand) and builds an aggregate demand function, as shown in Fig. 1. Using the aggregate demand function and the base price information π_k^{base} for that time period, the corresponding base aggregate demand d_k^{base} is determined. If $d_k^{\text{base}} < d^{\text{Feeder}}$ (see Fig. 1(a)) then $d_k^{\text{clr}} = d_k^{\text{base}}$ and $\pi_k^{\text{clr}} = \pi_k^{\text{base}}$. If $d_k^{\text{base}} \geq d^{\text{Feeder}}$ (see Fig. 1(b)) then $d_k^{\text{clr}} = d^{\text{Feeder}}$ and set π_k^{clr} accordingly.

The response (dispatch decision) of an individual DER to a transactive incentive signal (price signal) π_k^{clr} is given by,

$$v_{j,k} = \begin{cases} 0, & \text{if } \pi_{j,k} < \pi_k^{\text{clr}}, \\ 1, & \text{if } \pi_{j,k} \geq \pi_k^{\text{clr}}. \end{cases} \quad (4)$$

In this case of market-driven decisions, $u_{j,k}$ can be replaced by $v_{j,k}$ in (2).

C. DER Switching Logic including Lockout Constraint

In (2) and (4), no restrictions have been imposed on how frequently $u_{j,k}$ can switch on/off. This may lead to fast cycling,

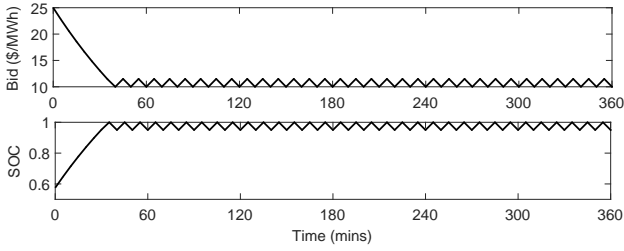


Fig. 2. Fast cycling when no lockout mode is present.

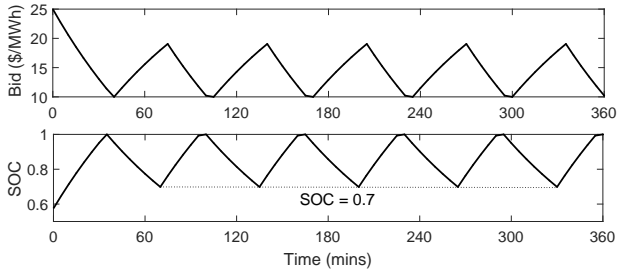


Fig. 3. Prolonged on/off periods in the presence of a lockout.

which is often undesirable. Fig. 2 provides an illustration where a DER's bid price was initially above the clearing price so it charged. With time, the SOC increases and its bid price decreases. Eventually the DER will reach full SOC or its bid price will drop below the market clearing price. When that occurs, the DER switches off, which caused its SOC and bid price to increase. Thus, its SOC and bid price oscillate within a narrow region. To avoid fast cycling when a DER is already fully charged, lockout constraints can be incorporated in the DER dispatch logic. For example, residential air conditioners employ hysteresis control to prevent fast cycling [9].

Let $m_{j,k}$ denote the locked-out (off)/ not-locked out (controllable) operating state. Then,

$$m_{j,k+1} = \begin{cases} 0, & \text{if } e_{j,k} \geq e_j^{\max}, \\ 1, & \text{if } e_{j,k} < e_j^{\text{set}}, \\ m_{j,k}, & \text{otherwise,} \end{cases} \quad (5)$$

which implies once the SOC reaches e_j^{\max} , the DER enters a locked out mode until its SOC drops below a user-defined level, e_j^{set} . Thus, the modified generalized battery equation becomes,

$$e_{j,k+1} = a_j e_{j,k} + \gamma_j v_{j,k} m_{j,k}. \quad (6)$$

It follows that each DER has the three operating states given in Table I. The effect of adding the lockout mode is shown in Fig. 3. Once reaching $e_{j,k} = e_j^{\max} = 1$ (full capacity), the DER remains off until its SOC falls below $e_{j,k} = 0.7$. Lockout conditions associated with e_j^{\min} can be modeled in a similar way.

D. Synchronization and Oscillations in TCL Simulation

Equations (2)-(6) governing DER operation were simulated for a population of (air conditioning) TCLs [9]. As illustrated

TABLE I
DER OPERATING STATES.

Op. state	$m_{j,k}$	$v_{j,k}$	Outcome
1	1	1	Controllable and cleared
2	1	0	Controllable, but not cleared
3	0	0	Locked and turned OFF

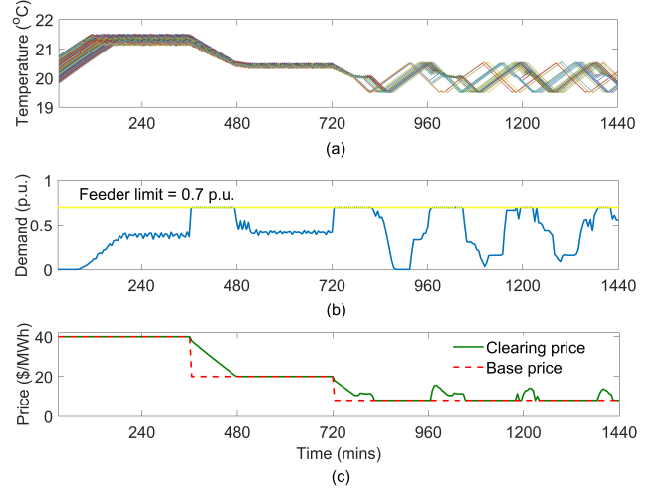


Fig. 4. (a) Temperature evolution of individual TCLs, (b) 5-minute average aggregate demand, (c) base price and clearing price [9].

in Fig. 4, the TCLs started with diverse initial temperatures. Because the base price remained high for a few hours, most of the TCLs did not consume power initially. Note that their temperatures became nearly synchronized at around 200 min. Later, as the base price dropped to 20 \$/MWh, almost all TCLs turned on. However, since the aggregate demand then exceeded $d^{\text{Feeder}} (= 0.7 \text{ p.u.})$, the clearing price increased. During minutes 480-720, the demand stayed flat. At 720 min, when the price dropped further, the TCLs found the low price even more favorable and consumed power. For TCLs reaching their minimum temperature, lockout conditions were activated resulting in prolonged on/off periods. Thus, large oscillations in the aggregate demand can be observed. A simplified aggregate model is presented next to provide further intuition.

E. Simplified Aggregate Model

When u_k is relaxed to be a continuous variable, $0 \leq u_k \leq 1$, (2) can express the average dynamics of a homogeneous population of devices [11]. In the context of a large aggregate storage device, u_k represents the normalized power consumption at time k [24]. Alternatively, u_k can be interpreted as the probability of being ON (charging). To establish an initial (simple) model, assume there is a proportional relationship between the bid price and the charging decision (i.e. higher bids provide a higher probability of being charged). Then,

$$u_k = K_p \pi_k, \quad (7)$$

where $K_p \geq 0$ is a proportional constant, which implicitly reflects the DER's bid strength relative to the market clearing

price. Let $K_p = 1/\pi^{\max}$. Then $\pi_k = \pi^{\max}$ will give $u_k = 1$. Substituting (3) into (7) and then using (2) gives,

$$u_{k+1} = (a - \gamma\beta K_p)u_k + \pi^{\max}K_p(1 - a). \quad (8)$$

Define $K_c = \pi^{\max}K_p(1 - a)$ and $\alpha = (a - \gamma\beta K_p)$. Then,

$$u_{k+1} = \alpha u_k + K_c, \quad (9)$$

which is a simple first order linear difference equation whose behavior is governed by underlying parameters γ , β and K_p . The solution to (9) can be written as,

$$u_k = \alpha^k u_0 + K_c \sum_{j=0}^{k-1} \alpha^j, \quad (10)$$

with equilibrium given by,

$$u^* = \frac{K_c}{1 - \alpha}, \quad e^* = \frac{\gamma\pi^{\max}K_p}{1 - \alpha}, \quad \pi^* = \frac{\pi^{\max}(1 - a)}{1 - \alpha}, \quad (11)$$

where $\gamma, \beta, K_p \geq 0$ and $\alpha \leq a$. Moreover, since $a < 1$ for any lossy battery, $\alpha < 1$. Stability conditions can easily be derived from (9). When $|\alpha| < 1$, the solution converges to the equilibrium u^* (i.e. the equilibrium is stable). When $0 < \alpha < a$ the solution is monotonic, whereas when $-1 < \alpha < 0$ the solution oscillates, with decreasing amplitude. Finally, when $\alpha < -1$, the solution oscillates with increasing amplitude, resulting in instability. This may occur with small values of a or with large values of γ , β or K_p . Thus, the bid curve slope β (also mentioned in [11]), a , γ and K_p all influence stability conditions.

For a numerical example, consider two cases:

- (i) $a = 0.9$, $\gamma = 0.1$, $\beta = 50$, $\pi^{\max} = 50$, $K_p = 0.02$, and
- (ii) $a = 0.7$, $\gamma = 0.25$, $\beta = 150$, $\pi^{\max} = 150$, $K_p = 0.05$.

For the first case, $\alpha = 0.8$ and the solution converges to $u^* = 0.5$, $e^* = 0.5$ and $\pi^* = 25$. In the second case, $\alpha = -1.175$ and the solution oscillates with increasing amplitude, ultimately diverging. This suggests that a collection of highly lossy DERs which have fast charging rates (e.g. poorly insulated houses with large AC units) and aggressive bid functions can negatively impact system stability.

Thus, (9) provides valuable insights into the response of a collection of homogeneous devices under transactive coordination. However, it assumes that u_k is a continuous variable, $0 \leq u_k \leq 1$, whereas the on/off decisions for individual DERs are discrete. Moreover, the effects of lockouts and feeder limits cannot be captured using (9).

F. Influence of Feeder Limit Constraints

Fig. 4 provides an example where the aggregate response of a group of DERs exhibits oscillatory behavior following synchronizing events. Under normal circumstances, each DER would turn on/off periodically during periods when the base price was low. Across a population of DERs, mixing of different frequency oscillations gives rise to damped oscillations and beating in the aggregate demand [9], [25], [26].

However, imposing a feeder capacity limit d^{Feeder} , as in Fig. 4, can affect the aggregate DER dynamics [9]. A drop in market price may lead to many DERs intending to charge simultaneously. When a strict feeder limit is imposed, only

the DERs with sufficiently high bids will initially be cleared. DERs with relatively lower bids wait until their bids rise sufficiently for them to be cleared. As a result, the DERs' on/off periods are affected by the feeder limit. Such a constraint can induce oscillations and beating, and may also lead to limit cycle behavior [25], [27], [28].

While transactive coordination can be influenced by a variety of phenomena (e.g. hysteresis, lockout, base price behavior and the feeder limit), a unified framework for studying such effects is lacking. Parametric studies using individual dynamic equations can be useful but cumbersome. Hence, efficient techniques for analyzing aggregate behavior are required. Economic and stable operation of the overall power system can be ensured by developing representative DER aggregate models and incorporating them into appropriate multi-period optimization problems.

III. AGGREGATE MODEL UNDER MARKET-BASED COORDINATION OF DERs

It has been shown in [12]–[15], [29], [30] that the natural dynamics of TCLs can be expressed in a bin model structure where each bin represents a temperature range and an on/off state. The evolution of the probabilities of TCLs lying in each bin can be described by,

$$X_{k+1} = AX_k, \quad (12)$$

where A is the transpose of the Markov transition matrix that is constructed from the probabilities associated with transitions between bins. It has been shown that the Markov transition matrix can be obtained analytically from the difference equations governing the TCL thermal dynamics [13], [15], [26], [31], or by applying system identification techniques [12], [13].

Existing bin-based aggregate models, however, do not capture the influence of transactive coordination on the behavior of DERs. There has also been limited attention given to synchronization issues. Hence, an aggregate model that incorporates price will now be developed. Lockout constraints and other mechanisms that eliminate synchronization will also be incorporated. This bin model is then used within an MPC framework in Section IV.

A. Homogeneous Population Model

The aggregate bin model expressing the dynamics of DERs (e.g. TCLs, storage devices, electric vehicles) under transactive coordination depends both on SOC dynamic equations and user bid curves. For a homogeneous population, the storage dynamic equation (2) becomes,

$$e_{j,k+1} = ae_{j,k} + \gamma u_{j,k}, \quad (13)$$

and the relationship (3) between bid price and SOC is,

$$\pi_{j,k} = \pi^{\max} - \beta e_{j,k}, \quad (14)$$

where the maximum bid is π^{\max} when $e_{j,k} = 0$ and the minimum bid is $\pi^{\min} = \pi^{\max} - \beta$ when $e_{j,k} = 1$. It is assumed that when $e_{j,k}$ reaches 1, the DER is automatically switched off.

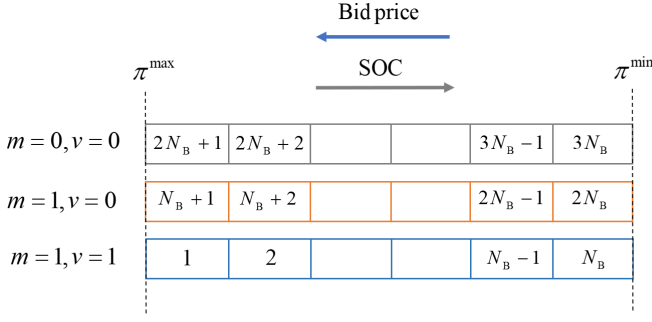


Fig. 5. Bin model for a homogeneous population. Bid prices decrease from left to right whereas SOC levels increase. The three different operating states are marked on the left.

Assume market clearing occurs every τ minutes, during which it is reasonable to assume there would be discrete shifts in the SOC levels and the price bids. Consider N_B bins (i.e. discrete price intervals) between π^{\max} and π^{\min} , with each bin's width being $(\pi^{\max} - \pi^{\min})/N_B$. The bins have indices $i = 1, \dots, N_B$. The bins are organized by decreasing price levels, with $\tilde{\pi}_0 = \pi^{\max}$ and $\tilde{\pi}_{N_B} = \pi^{\min}$. The i -th bin's boundaries are $\{\tilde{\pi}_{i-1}, \tilde{\pi}_i\}$. For a homogeneous model, a direct mapping to the discrete SOC levels can be obtained. Let \tilde{e}_i , $i = 0, 1, \dots, N_B$, be the discrete SOC levels associated with $\tilde{\pi}_i$, so that $\tilde{e}_0 = e^{\min} = 0$ and $\tilde{e}_{N_B} = e^{\max} = 1$.

Note that each bin also needs to consider the on/off and locked status outlined in Table I. Hence, a three-stage bin model is proposed, as illustrated in Fig. 5, where bins are mapped to the operating states by defining the sets,

$$I_1 = \{1, \dots, N_B\} \quad \text{for } m = 1, v = 1 \quad (15a)$$

$$I_2 = \{N_B + 1, \dots, 2N_B\} \quad \text{for } m = 1, v = 0 \quad (15b)$$

$$I_3 = \{2N_B + 1, \dots, 3N_B\} \quad \text{for } m = 0, v = 0. \quad (15c)$$

Let $x_{i,k} \geq 0$ be the fraction of DERs lying inside bin i at time k , where $i \in I_1, I_2$ or I_3 , depending on the bid price (or the SOC level) and the operating state. Let $p_{j,i}$ be the probability of transitioning from bin j to bin i in one time step. Then the state transitions for the i -th bin can be written,

$$x_{i,k+1} = \sum_{j=1}^{3N_B} p_{j,i} x_{j,k}, \quad \forall i, k. \quad (16)$$

This can be expressed in matrix form (12) as,

$$A = \begin{bmatrix} p_{1,1} & p_{1,2} & \cdots & p_{1,3N_B} \\ p_{2,1} & p_{2,2} & \cdots & p_{2,3N_B} \\ \vdots & \vdots & \ddots & \vdots \\ p_{3N_B,1} & p_{3N_B,2} & \cdots & p_{3N_B,3N_B} \end{bmatrix}^T. \quad (17)$$

Note that $0 \leq p_{j,i} \leq 1$, $\forall i, j$, and $\sum_{i=1}^{3N_B} p_{j,i} = 1$, $\forall j$.

Assume the clearing price is π_k^{clr} . Then, all TCLs in bins with bid prices greater than π_k^{clr} will be cleared. For a fixed value of π_k^{clr} , the transition probabilities $p_{j,i}$ can be estimated from a large number of samples by observing the evolution of DERs after the market clears at τ minutes.

The clearing price π_k^{clr} determines which bins are cleared. Hence, the $p_{j,i}$ are functions of π_k^{clr} and the A -matrix is time-varying for varying π_k^{clr} . The aggregate model can be expressed as,

$$X_{k+1} = A_k X_k. \quad (18)$$

If π_k^{clr} remains constant then $A_k = A, \forall k$. Section V-B illustrates the construction of the A -matrices, the connection between system behavior and the eigenvalues of A_k , and model performance.

B. Bin Model under Parameter Heterogeneity

When parameters are heterogeneous, bins are defined similarly to Section III-A, except $\tilde{\pi}_0 = \max \pi_j^{\max}$ and $\tilde{\pi}_{N_B} = \min \pi_j^{\min}$. Compared to the homogeneous case, however, the discretization in SOC levels cannot be mapped directly to the bid price levels, unless additional bins are added to track both SOC levels and bid prices. The A -matrix elements can be obtained from a large number of samples. Alternatively, the dynamics of the heterogeneous population can be captured by considering clusters of homogeneous groups and their respective transition equations [26], [32].

C. Reformulation of the Transition Equations

While (18) can be used to simulate the aggregate behavior of DERs, the price signal must be known *a priori*. To determine the optimal price signal and resultant cleared demand in a multi-period optimization problem, the influence of price variation must be separated from the propagation dynamics (12). This can be accomplished by decomposing the state associated with each bin into ON and OFF fractions,

$$x_{i,k} = x_{i,k}^{\text{on}} + x_{i,k}^{\text{off}}, \quad x_{i,k}^{\text{on}}, x_{i,k}^{\text{off}} \geq 0, \quad \forall i \in I_1 \cup I_2, \forall k, \quad (19)$$

where $x_{i,k}^{\text{on}}$ and $x_{i,k}^{\text{off}}$ are decision variables determined by the optimization process. More specifically, the division between ON and OFF fractions of a bin is determined by a comparison between the bid price associated with that bin and the clearing price π^{clr} .

Given values for the decision variables $x_{i,k}^{\text{on}}$ and $x_{i,k}^{\text{off}}$, the states are reset according to,

$$x_{i,k}^+ = x_{i,k}^{\text{on}} + x_{i+N_B,k}^{\text{on}}, \quad \forall i \in I_1, \forall k, \quad (20a)$$

$$x_{i,k}^+ = x_{i,k}^{\text{off}} + x_{i-N_B,k}^{\text{off}}, \quad \forall i \in I_2, \forall k, \quad (20b)$$

where the '+' superscript indicates reset values. Note also that for the locked bins, $i \in I_3$, no DERs can be turned on. Hence,

$$x_{i,k}^+ = x_{i,k} = x_{i,k}^{\text{off}}, \quad \forall i \in I_3, \forall k. \quad (21)$$

These reset equations can be expressed in matrix form,

$$X_k^+ = B^{\text{on}} X_k^{\text{on}} + B^{\text{off}} X_k^{\text{off}}. \quad (22)$$

Starting from the reset state values, the evolution of the bin probabilities has a similar form to (12),

$$X_{k+1} = A X_k^+, \quad (23)$$

where A now captures the natural dynamics of DERs, as expressed by (13) and (14).

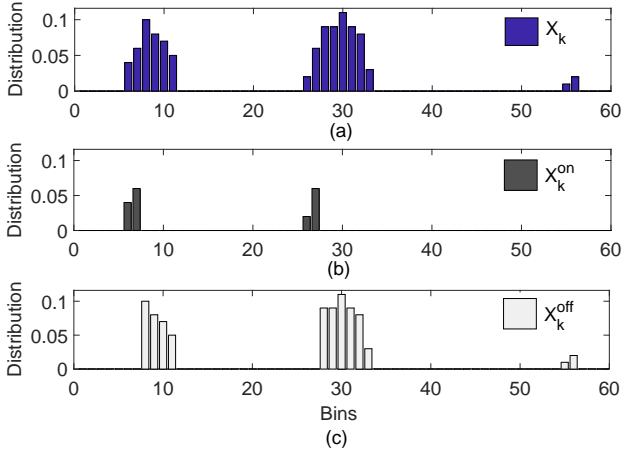


Fig. 6. Distributions for (a) X_k , (b) X_k^{on} and (c) X_k^{off} .

Finally, it should be noted that the structure of A ensures conservation of probability,

$$\sum_{i=1}^{3N_B} x_{i,k} = 1, \quad \forall k, \quad (24)$$

and $x_{i,k} \geq 0, \forall k$. Note that with this reformulation all equations remain linear. This is especially helpful for MPC design, as shown in Section IV.

An example with $N_B = 20$ (total 60 bins) is shown in Fig. 6. Bins lie in three sets $I_1 = \{1, \dots, 20\}$, $I_2 = \{21, \dots, 40\}$, and $I_3 = \{41, \dots, 60\}$. The overall distribution, X_k at time k , is shown in Fig. 6(a). Recall from the bin definitions and from Fig. 5 that bins from left to right have decreasing bid prices. Also, while I_1, I_2, I_3 differ in their operating states, the bid prices at bins $i, i + N_B$ and $i + 2N_B$, where $i = 1, \dots, 20$, are the same. Assume, $\pi_k^{\text{clr}} = \tilde{\pi}_7$. Thus, all DERs in bins 6, 7, 26 and 27 are cleared. The ON and OFF distributions, $X_k^{\text{on}}, X_k^{\text{off}}$, are shown in Figs. 6(b) and 6(c). By (22),(23), B^{on} and B^{off} will then act on X_k^{on} and X_k^{off} , respectively, to give X_{k+1} .

D. Logic Equations for Market Clearing

An arbitrary optimizer could choose the ON/OFF quantities from each bin as long as (19)-(24) were satisfied. However, in a transactive dispatch mechanism, DERs with higher bid prices than the clearing price are cleared. Hence, additional logic is required to simulate behavior under the transactive market clearing mechanism. For example, with the bin definitions of Fig. 5, bins from right to left have increasing bid prices, and so should have higher priority to turn on. To accomplish this, binary variables can be used.

Let $u_{i,k}^{\text{on}} \in \{0, 1\}$ be the binary on/off decision associated with clearing all TCLs in bin i , and consider the following set

of equations:

$$0 \leq x_{i,k}^{\text{on}} \leq u_{i,k}^{\text{on}}, \quad i = 1, \dots, 2N_B \quad (25a)$$

$$0 \leq x_{i,k}^{\text{off}} \leq u_{i,k}^{\text{off}}, \quad i = 1, \dots, 3N_B \quad (25b)$$

$$u_{i,k}^{\text{on}} + u_{i,k}^{\text{off}} = 1, \quad i = 1, \dots, 3N_B \quad (25c)$$

$$u_{i,k}^{\text{on}} \geq u_{i+1,k}^{\text{on}}, \quad i = 1, \dots, N_B - 1 \quad (25d)$$

$$u_{i,k}^{\text{on}} = u_{i+N_B,k}^{\text{on}}, \quad i = 1, \dots, N_B. \quad (25e)$$

If $x_{i,k}^{\text{on}}$ DERs from bin i are to be chosen to be ON, we need $u_{i,k}^{\text{on}} = 1$, otherwise $u_{i,k}^{\text{on}} = 0$. This is accomplished by (25a). Likewise, by (25b), $u_{i,k}^{\text{off}} \in \{0, 1\}$ is used for choosing $x_{i,k}^{\text{off}}$. Ensuring that each bin has only ON or OFF DERs is achieved by (25c). (We assume that when a bin is cleared, all DERs in that bin turn on.) Next, (25d) ensures that bins with higher bid prices must be turned ON before bins with lower prices can be chosen. Finally, (25e) ensures that bins with the same bid prices, but different operating states I_1 and I_2 get cleared simultaneously. Note that the logic equations (25a)-(25e) are linear in $x_{i,k}^{\text{on}}, x_{i,k}^{\text{off}}, u_{i,k}^{\text{on}}$, and $u_{i,k}^{\text{off}}$.

IV. MODEL PREDICTIVE CONTROL FORMULATION

The bin-based aggregate model of DERs can be incorporated into a model predictive control framework to determine the DER schedule that gives minimum power supply cost over a finite horizon. Let the distribution network be supplied by power sources P_k^s , $s = 1, \dots, N_s$ at time k . Each source has cost $C_s(P_k^s)$ which is typically quadratic. The overall demand of the network at time k is D_k , which is composed of controllable DER demand D_k^c and uncontrollable demand D_k^o of other loads. The cost minimization problem can be formulated as,

$$\min \sum_{k=1}^{N_k} \sum_{s=1}^{N_s} C_s(P_k^s) \quad (26a)$$

$$\text{s.t.} \quad \sum_{s=1}^{N_s} P_k^s = D_k, \quad \forall k \quad (26b)$$

$$D_k = D_k^c + D_k^o, \quad \forall k, \quad (26c)$$

$$D_k^c = \sum_{i=1}^{3N_B} x_{i,k}^{\text{on}}, \quad \forall k, \quad (26d)$$

$$x_{i,k=1} = x_i^{\text{ini}}, \quad \forall i, \quad (26e)$$

$$D_k \leq d^{\text{Feeder}} \quad \forall k, \quad (26f)$$

along with the transition equations (19)-(24) and logic constraints (25a)-(25e).

The objective function (26a) minimizes the total cost of supply. Supply-demand balance is enforced by (26b). The Lagrange multiplier associated with this constraint represents the electricity price, λ_k^{elec} . Total demand is established by (26c), with (26d) relating aggregate controllable load to the ON fractions of all bins. Initial conditions are established by (26e), where X^{ini} is assumed to be known. Finally, (26f) ensures the feeder limit is not violated. Individual capacity and ramp limits for each supplier may also be incorporated.

Additionally, to avoid arbitrarily setting $u_{i,k}^{\text{on}} = 1$, a cost $\tilde{C}_i(u_{i,k}^{\text{on}})$ is included in the objective,

$$\sum_{k=1}^{N_k} \sum_{s=1}^{N_s} C_s(P_k^s) + \mu_w \sum_{k=1}^{N_k} \sum_{i=1}^{3N_B} \tilde{C}_i(u_{i,k}^{\text{on}}), \quad (27)$$

where μ_w is a tuning parameter. Note, $\tilde{C}_i(u_{i,k}^{\text{on}}) = 1, \forall i, k$ has been used in this paper.

Due to the presence of both continuous and binary variables, the overall formulation is a mixed integer programming (MIP) problem. A mixed integer linear program (MILP) can be obtained by approximating the suppliers' quadratic cost functions with piecewise linear segments.

A. Measures to Avoid DER Synchronization

Synchronization occurs when a large fraction of DERs lie within a narrow range of bins. It may lead to large oscillations in the aggregate demand and high volatility in clearing prices. Hence, to avoid this situation, let b^{max} be the maximum allowable fraction in any bin, and enforce the constraint,

$$x_{i,k} \leq b^{\text{max}}, \quad \forall i, k. \quad (28)$$

Alternatively, a quadratic cost term can be added in the objective function,

$$\sum_{k=1}^{N_k} \sum_{s=1}^{N_s} C_s(P_k^s) + \mu_w \sum_{k=1}^{N_k} \sum_{i=1}^{3N_B} \tilde{C}_i(u_{i,k}^{\text{on}}) + \mu_s \sum_{i=1}^{3N_B} (x_{i,k} - b^{\text{avg}})^2, \quad (29)$$

where $b^{\text{avg}} = 1/(3N_B)$ and μ_s can be adjusted to distribute DERs widely over the bin space.

B. QP Formulation

Instead of using binary variables in (25a)-(25e) and (27), a relaxed QP formulation can be established by assigning costs per bin, $\hat{C}_i(x_{i,k}^{\text{on}})$, that increase with increasing bin index. For example, $\hat{C}_i(x_{i,k}^{\text{on}}) = w_o^i x_{i,k}^{\text{on}}, \forall i \in I_1$ and $\hat{C}_i(x_{i,k}^{\text{on}}) = w_o^{i-N_B} x_{i,k}^{\text{on}}, \forall i \in I_2$, where $w_o > 1$. (The simulations in Section V use $w_o = 3$.) The modified objective function becomes,

$$\sum_{k=1}^{N_k} \sum_{s=1}^{N_s} C_s(P_k^s) + \mu_w \sum_{k=1}^{N_k} \sum_{i=1}^{3N_B} \hat{C}_i(x_{i,k}^{\text{on}}) + \mu_s \sum_{i=1}^{3N_B} (x_{i,k} - b^{\text{avg}})^2, \quad (30)$$

where μ_w is a tuning parameter.

The overall formulation consists of the objective (30), constraints (26b)-(26f) and transition equations (19)-(24). All constraints become linear and the objective function remains quadratic. Overall, we obtain an efficient QP form.

C. Transactive Dispatch Rule

Once the above problem has been solved, the indices of the ON bins can be recovered from $x_{i,k}^{\text{on}}$ or $u_{i,k}^{\text{on}}$. Define i_k^{max} as the largest index among the ON bins at period k (for $i \in I_2$ subtract N_B from bin indices). For the MIP solution,

$$i_k^{\text{max}} = \max_i \{u_{i,k}^{\text{on}} = 1\}, \quad \forall k. \quad (31)$$

Since u^{on} does not appear in the QP formulation, in that case a bin is considered to be cleared when $x_{i,k}^{\text{on}}$ is larger than a threshold ζ ,

$$i_k^{\text{max}} = \max_i \{x_{i,k}^{\text{on}} \geq \zeta\}, \quad \forall k. \quad (32)$$

From the SOC-bin mapping of Fig. 5, the price associated with i_k^{max} becomes the clearing price π_k^{clr} , that is broadcast to all the DERs for time period k . Upon receiving this price, all

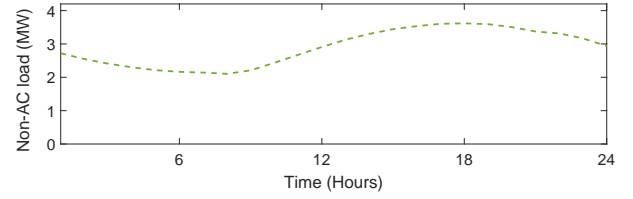


Fig. 7. Aggregate demand profile excluding air-conditioner (AC) demand.

DERs in bins $i \leq i_k^{\text{max}}$, (i.e. bins with higher bid prices) should dispatch,

$$u_{j,k} = \begin{cases} 1, & \text{if } \pi_{j,k} \geq \tilde{\pi}_k^{\text{max}}, \\ 0, & \text{if } \pi_{j,k} < \tilde{\pi}_k^{\text{max}}. \end{cases} \quad (33)$$

D. Practical Considerations

Assume all DERs are managed by a single aggregator in a distribution system. To obtain X^{ini} , which is required for (26e), an aggregator could collect local measurements from DERs typically near the end of an MPC horizon. Each DER's on/off, locked status and its associated bid price are used to construct X^{ini} . Since only aggregate information is needed, each DER sends updates anonymously. Assuming a distribution system operator (DSO) solves the MPC, the aggregator would send X^{ini} to the DSO. The DSO also has access to the A -matrix of (23), which the aggregator estimates separately. The DSO solves the MPC and sends the aggregator the clearing prices $\pi_k^{\text{clr}}, k = 1, \dots, N_k$. The price π_k^{clr} can be revealed to DERs either just for the next market clearing interval or for several periods ahead, depending on communication bandwidth availability. Since MPC already accounts for the feeder limit, the two-step market clearing process described in Section II-B is not necessary. However, if the mechanism in Section II-B is followed, individual DER bids additionally need to be collected at every market clearing interval.

V. SIMULATION RESULTS

A. Data

The case study considers a typical distribution system serving predominantly residential loads (1,473 customers) located in Austin, TX [17]. The system peak demand was recorded at 7.77 MW. Energy usage analysis of real data from 88 single-family houses in the Mueller neighborhood of Austin, from July 2012 to June 2013, was undertaken in [33]. It was found that approximately 47% of the peak household demand was consumed by air-conditioner (AC) units during summer peak days. Based on this analysis and hourly demand data from the Electric Reliability Council Of Texas (ERCOT) [34], the non-AC demand profile of Fig. 7 was estimated. Since each AC consumes approximately 3 kW on average (see Appendix VII-A), the maximum AC load can be up to 4.4 MW, which would result in a peak demand exceeding 8 MW.

B. Aggregate Model Performance

To study the performance of the aggregate model (18), first the A -matrix coefficients need to be obtained. Consider a

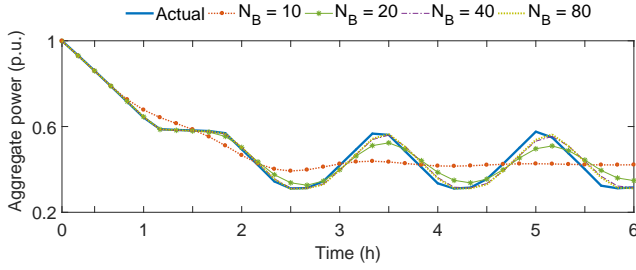


Fig. 8. Aggregate demand profiles, for varying N_B , with clearing price at 10 \$/MWh (TCL initial temperatures uniform within 19 to 21°C).

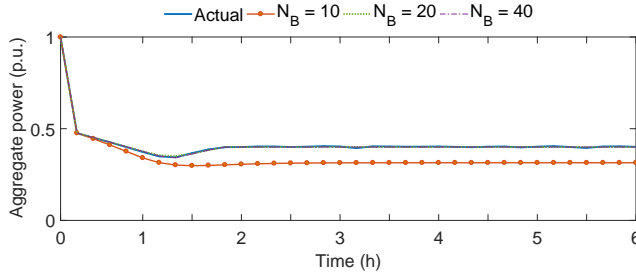


Fig. 9. Aggregate demand profiles, for varying N_B , with clearing price at 30 \$/MWh (TCL initial temperatures uniform within 19 to 21°C).

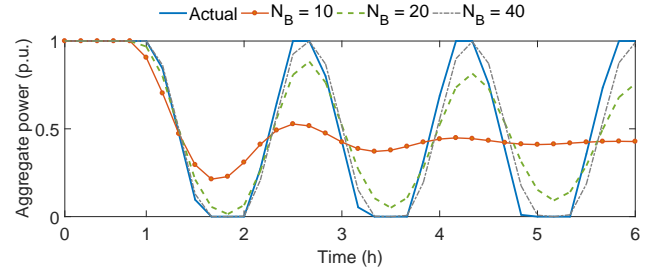


Fig. 10. Aggregate demand profiles, for varying N_B , with clearing price at 10 \$/MWh (TCL initial temperatures uniform within 19.8 to 20.2°C).

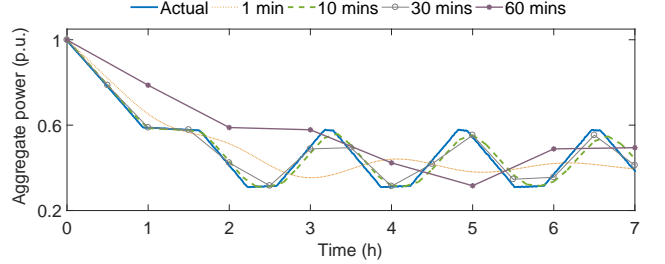


Fig. 11. Aggregate demand profiles, for varying market clearing intervals, with $\pi^{\text{clr}} = 10$ \$/MWh (Initial temperatures uniform within 19-21°C).

homogeneous population with $\beta_j = 40$ \$/MWh, $\pi_j^{\text{max}} = \$50$, $\forall j$. With $\tau = 10$ min and known price signals, 1000 TCLs were simulated. For TCLs originating in a specific sending bin, we can find the range of bins reached by TCLs at the end of 10 minutes. Repeating for all bins and normalizing these quantities, the transition probabilities (thus, the A -matrix) for a known price signal were obtained.

First, consider $\pi^{\text{clr}} = 10$ \$/MWh. All TCLs have bids just above the clearing price, hence can get cleared. The aggregate power consumed by 1000 TCLs over 6 hours has been shown in Fig. 8. Note that the initial temperatures of TCLs were distributed uniformly between 19 to 21°C. With $\tau = 10$ minutes, the aggregate behavior was also simulated using bin models of various orders, $N_B = 10, 20, 40, 80$. With $N_B = 10$ the aggregate demand profile deviates significantly from the actual. The profiles obtained with the other models matched the actual reasonably well. Fig. 9 shows the performance for varying N_B when $\pi^{\text{clr}} = 30$ \$/MWh. Again, the profile obtained using the $N_B = 10$ model deviates from the actual.

Next, the A -matrix obtained for 10 \$/MWh was used to simulate the aggregate demand with initial temperatures of TCLs distributed uniformly between 19.8 and 20.2°C. Profiles are shown in Fig. 10. Since most TCLs turned on/off almost at the same time, the oscillation amplitudes were larger compared to those in Fig. 8.

With the price signal fixed at $\pi^{\text{clr}} = 30$ \$/MWh, the aggregate demand reaches a constant level, whereas with $\pi^{\text{clr}} = 10$ \$/MWh, oscillatory behavior has been observed. This is because with a low clearing price, TCLs enter the locked mode when their temperatures reach 19°C and again become controllable when temperatures exceed 19.6°C. Analyzing the

eigenvalues of the A -matrices, we observed that for the A -matrix with $\pi^{\text{clr}} = 30$ \$/MWh, the eigenvalues have only real parts. For the A -matrix with $\pi^{\text{clr}} = 10$ \$/MWh, pairs of complex eigenvalues exist, suggesting an oscillatory response. Ideally under $\pi^{\text{clr}} = 10$, a homogeneous population exhibits undamped oscillations, whereas the eigenvalues of the A -matrix suggest damped oscillations. This discrepancy exists due to modeling error from the discretization [12], [26], [35]. However, as shown in Figs. 8 and 10, with sufficiently large N_B the actual behavior can be tracked closely for several hours, which is suitable for control purposes [26], [35].

The effect of changing the market clearing interval τ is analyzed next. Consider $\tau = 1, 10, 30$ and 60 minutes. The A matrices, with $N_B = 40$, were obtained for each case under $\pi^{\text{clr}} = 10$ \$/MWh. As shown in Fig. 11, with $\tau = 10$ min, the profile obtained by (18) deviates from the actual. This is because with a smaller τ , the small changes in temperature (or bids) can only be accurately captured by using large N_B [13], [26], [29], and using $N_B = 40$ is not sufficient. The profile obtained with $\tau = 10, 30$ minutes match the actual behavior reasonably well. With $\tau = 60$ minutes, the profile again deviates significantly. During the duration of 60 minutes, many TCLs reach their temperature thresholds and change state. Hence, the 60 minute bin model could not capture the intra-hour power consumption dynamics.

C. MPC Performance

Consider $\tau = 10$ min, and $N_B = 20$. Cost of supply, $C_k^s(P_k^s) = 10P_k^s + 2.5(P_k^s)^2$. The substation feeder limit is set at 8 MW.

For a storage based system, deciding only based on current or near-term situations may lead to significant reduction of the

TABLE II
PERFORMANCE COMPARISON

Set up	Case 1	Case 2	Case 3	Case 4	Case 5	Case 6	Case 7	Case 8
MPC type	MIP	MIP	MIP	MIP	QP	QP	QP	QP
Horizon, N_k	12	12	18	18	18	18	18	18
b^{\max}	1	0.25	1	1	0.25	0.15	0.25	0.25
Tuning parameter, μ_s	0	0	0	1000	1000	1000	1000	1000
Tuning parameter, μ_w	1	1	1	1	200	200	200	200
Results								
Average system demand, \bar{D}_k , in MW	4.82	7.10	4.74	6.08	4.68	4.74	4.68	4.68
Average TCL demand, \bar{D}_k^c , in MW	1.30	3.87	1.28	2.62	1.21	1.28	1.21	1.21
Peak system demand, \hat{D}_k , in MW	5.20	8.00	5.19	8.00	5.20	6.78	5.21	5.21
RMSE (normalized), in %	0.82	1.19	0.79	0.72	3.22	7.88	3.16	3.89
$\bar{\lambda}_k^{\text{elec}}$ (average electricity price), in \$/MWh	34.1	47	33.7	40.4	33.4	33.7	33.4	33.4
$\lambda_k^{\text{elec-}}$, $\lambda_k^{\text{elec+}}$ (min, max), in \$/MWh	30.2, 36.5	38.5, 50	30, 35.9	26.7, 50.2	30.7, 34.8	29.4, 35.8	30.8, 34.6	30.7, 34.8
Maximum TCLs in a single bin, in %	0.41	0.25	0.39	0.16	0.25	0.15	0.25	0.25
Bin spread at X_{N_k}	5	13	5	12	12	11	12	12

feasible operating region in future periods [15], [31]. Hence, we look ahead several periods in the MPC. Consider $N_k = 18$. With $\tau = 10$ min, the MPC looks ahead a 3 hour window (2 hours in cases 1 and 2). Additionally, let $\sum_{k=1}^{N_k} D_k^c \geq 1.21N_k$, where 1.21 MW is an average aggregate TCL demand allowed to avoid the depletion of the aggregate SOC.

Recall that MPC requires the A -matrix. To obtain the coefficients of A , distribute TCLs uniformly over all bins. For TCLs originating from each sending bin, find the range of bins covered at the end of $\tau = 10$ minutes. Normalizing these quantities gives the transition probabilities. Recall that this matrix is not a function of the clearing price, hence is valid under any clearing price signal.

Both the QP and MIP problems were programmed in MATLAB and YALMIP [36]. QP problems (cases 5-8) were solved using Quadprog, whereas the MIPs (Cases 1-4) were solved using Gurobi. For validation, in each case we ran the full dispatch of 1473 TCLs to test the performance of the MIP/QP solutions. Due to space limitations, only results for tests starting from hour 18 have been presented. Test parameters and results are summarized in Table II. The average system demand, \bar{D}_k , average TCL demand, \bar{D}_k^c , and system peak demand \hat{D}_k are shown. Also, the average, minimum and maximum price of electricity, $\bar{\lambda}_k^{\text{elec}}$, $\lambda_k^{\text{elec-}}$, and $\lambda_k^{\text{elec+}}$, were recorded. The error between the scheduled and the actual system demand during the dispatch process is captured by the root mean square error (RMSE) (here, normalized by the system peak capacity of 8 MW). Initially, temperatures of TCLs were distributed uniformly within 20 to 21°C. To measure synchronism, maximum TCLs in a single bin (%) in $X_k, \forall k$, and the bin spread (i.e. the number of bins with non-zero quantities of TCLs) in X_{N_k} were recorded. The following observations are made,

- In cases 1 and 3, $b^{\max} \leq 1$ (i.e. all TCLs can be in a single bin) and $\mu_s = 0$, hence the risk of synchronization was not accounted for. As a result, X_{N_k} was narrowly distributed over 5 bins only. Also, the maximum fraction of TCLs in a single bin reached approximately 40%.
- Measures to avoid synchronization were taken by setting $b^{\max} \leq 0.25$ in case 2, and by $\mu_s = 1000$ in case 4. Maximum TCLs lying in a single bin decreased considerably and

wider X_{N_k} were obtained. However, \bar{D}_k^c , \hat{D}_k and $\bar{\lambda}_k^{\text{elec}}$ were significantly higher in cases 2 and 4.

- In case 5, applying the QP solution, the obtained \bar{D}_k^c , \hat{D}_k and $\bar{\lambda}_k^{\text{elec}}$ were similar to the values in case 3. The demand profiles (and λ_k^{elec}) obtained in cases 3 and 5 are shown in Fig. 12. However, the RMS error was higher in case 5. This is because the QP does not need to enforce strict on/off decisions for the entire bin, whereas the MIP does. Under QP, contents in a bin can be fractionally chosen to be on. However, during dispatch, all TCLs in that bin are cleared due to receiving the same price signal. This causes the actual profile to slightly deviate from the predicted one.
- In case 6, when a stricter b^{\max} limit was imposed than in case 5, \bar{D}_k^c and $\bar{\lambda}_k^{\text{elec}}$ slightly increased. RMSEs and \hat{D}_k , however, increased noticeably. Again, this was mostly due to the QP solutions favoring fractional ON quantities in a bin in order to meet lower b^{\max} , which eventually led to higher error during the dispatch.
- In case 7, noise (uniform $[-0.02, 0.02]$, in °C/min) was introduced in the model, affecting the temperature dynamics of the TCLs. The bin model was identified under noisy data. During the dispatch process, the RMSE did not increase, rather results were comparable to case 5.
- In case 8, bid slopes were heterogeneous (uniform [36, 44], in \$/MWh). While the cost of the solution (i.e. $\bar{\lambda}_k^{\text{elec}}$) remained nearly the same, the RMSE increased slightly. This can be attributed to the bin model's reduced accuracy to deal with parameter heterogeneity. Model performance could worsen further when considering heterogeneity in other TCL parameters [26]. This could be better modeled by using clusters of homogeneous groups [26], [32].

Additionally, it was noted that the average time taken to solve the MPCs were 95 s for MIPs with $N_k = 18$, 23 s for MIPs with $N_k = 12$, and less than 2 s for all QP problems.

D. Discussions

Comparing the MIP and QP solutions in Table II, in general, we observe that the average TCL demand, peak demand and average electricity prices with QP were lower compared to the results obtained by the MIP. However, the QP solutions

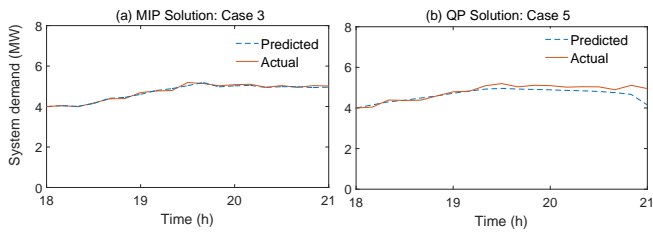


Fig. 12. Predicted and actual system demand profiles using (a) MIP in case 3, and (b) QP in case 5.

typically lead to higher error (i.e. RMSEs values). To reduce the error during the dispatch process, alternative dispatch schemes could be sought in future work. Discriminatory prices or incentive signals could be sent to the TCLs. For example, each TCL could receive a clearing price that is slightly perturbed by noise. This could potentially reduce the RMSE, however, detailed investigation should be carried out to analyze the effectiveness and the fairness of such schemes.

To reduce the likelihood of an oscillatory response and to lower error during the dispatch, we included $\mu_s > 0$ in the objective or imposed b^{\max} . Due to the large degree of freedom when using the QP formulation, the above strategies typically did not increase the cost of the solution (except in case 6). The more restrictive MIP form typically led to higher cost solutions, especially for high μ_s or low b^{\max} .

Our framework was shown to effectively relieve congestion at a substation feeder by looking ahead several hours. While for slowly varying systems, such as EVs and commercial building HVAC systems, hourly time steps have been used in several recent studies [18], [19], [37], [38], 10 minute price signals have been used to capture the dynamics of TCLs in our case. Future work could apply our proposed framework in a rolling horizon setting and for other power system applications. One natural extension could be to deal with network congestion. Recent work investigates distribution locational marginal prices (LMPs) to alleviate network congestion while considering dynamics of EVs [37], [38] and HVACs [18], [19]. Compared to these approaches, our method has the advantage that it lets users choose their individual bid functions and the aggregator makes decisions utilizing the bin-based aggregate model. One could consider aggregating loads at different nodes of the network, which will then allow computing the nodal LMPs and the optimal incentive signals for each aggregation.

VI. CONCLUSIONS

Recent studies have shown that transactive coordination of DERs, such as TCLs, batteries, and EVs, can lead to undesirable power oscillations. In this paper, we analyzed the causes of such oscillations and identified different factors that can affect the aggregate DER dynamics. The user defined bid slopes, preference for setting locking conditions, price signals sent to DERs for coordinating their responses, and imposing feeder limits, all can affect the natural charging and discharging cycles of DERs, hence can lead to load synchronization and undesired power oscillations. To address these issues, we

developed a bin-based DER aggregate model under transactive coordination. The trade-offs when using varying model orders and market intervals were analyzed. With reformulation of the transition equations, we showed how the model can be incorporated in an MPC framework. The MPC can then be solved to find optimal price signals that should be sent to the DERs for governing their aggregate responses in a desired manner. An accurate MIP formulation, and a relaxed QP formulation have been developed and tested. Simulation results compared the performance under several different scenarios by varying the initial conditions, penalty for synchronization, noise and heterogeneity. Future work could involve extending our approach to study hierarchical coordination among system operators, DSOs and aggregators. Schemes that can consider non-uniform incentive signals could also be investigated.

VII. APPENDICES

A. TCL Model

The internal and ambient temperatures ($^{\circ}\text{C}$) corresponding to each TCL load j are denoted by θ_j and θ^a , respectively. Each load can be modeled as a thermal capacitance, C_j ($\text{kWh}/^{\circ}\text{C}$), in series with a thermal resistance, R_j ($^{\circ}\text{C}/\text{kW}$). The binary variable m_j denotes the on/off status of the load, and P_j (kW) is the energy transfer rate when a cooling (or heating) TCL is switched ON. The dynamics of a TCL's temperature can be modeled using a first-order difference equation [39], [40],

$$\theta_{j,k+1} = \tilde{a}_j \theta_{j,k} + (1 - \tilde{a}_j)(\theta^a - m_{j,k} \theta_j^g), \quad (34)$$

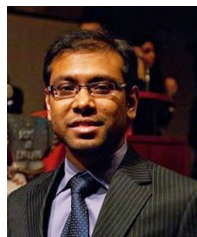
where the time between k and $k+1$ is h (in our simulation, $h = 10$ s), $\tilde{a}_j = e^{-h/(C_j R_j)}$ is the parameter governing the thermal characteristics of the thermal mass, and $\theta_j^g = P_j R_j$ is the temperature gain when a cooling TCL is ON. The variable $m_{j,k}$ switches off when $\theta_{j,k} < \theta_j^{\min}$ and on when $\theta_{j,k} > \theta_j^{\max}$. Comparing with the battery model in (2), $e_j = 1$ when $\theta_{j,k}$ reaches θ_j^{\min} and $e_j = 0$ when $\theta_{j,k}$ reaches θ_j^{\max} . With coefficient of performance (COP) η_j , the electrical power consumed is given by, $P_{j,k}^{\text{elec}} = m_{j,k} P_j / \eta_j$.

Following the calculation procedure in [41], for a 176 m^2 house with 3 ton (approximately 10.55 kW) AC [33] and $\eta_j = 3.5$, the parameters would be $P_j^{\text{elec}} = 3 \text{ kW}$ when on, $R_j = 2.84^{\circ}\text{C}/\text{kW}$, and $C_j = 7.04 \text{ kWh}/^{\circ}\text{C}$.

REFERENCES

- [1] P. Huang, J. Kalagnanam, R. Natarajan, M. Sharma, R. Ambrosio, D. Hammerstrom, and R. Melton, "Analytics and Transactive Control Design for the Pacific Northwest Smart Grid Demonstration Project," in *IEEE SmartGridComm*, 2010, pp. 449–454.
- [2] J. C. Fuller, K. P. Schneider, and D. Chassin, "Analysis of residential demand response and double-auction markets," in *IEEE Power and Energy Society General Meeting*, 2011, pp. 1–7.
- [3] S. Li, W. Zhang, J. Lian, and K. Kalsi, "Market-Based Coordination of Thermostatically Controlled LoadsPart I: A Mechanism Design Formulation," *IEEE Transactions on Power Systems*, vol. 31, no. 2, pp. 1170–1178, 2016.
- [4] —, "Market-Based Coordination of Thermostatically Controlled LoadsPart II: Unknown Parameters and Case Studies," *IEEE Transactions on Power Systems*, vol. 31, no. 2, pp. 1–9, 2016.

- [5] J. Knudsen, J. Hansen, and A. M. Annaswamy, "A Dynamic Market Mechanism for the Integration of Renewables and Demand Response," *IEEE Transactions on Control Systems Technology*, vol. 24, no. 3, pp. 940–955, 2016.
- [6] H. Hao, C. D. Corbin, K. Kalsi, and R. G. Pratt, "Transactive control of commercial buildings for demand response," *IEEE Transactions on Power Systems*, vol. 32, no. 1, pp. 774–783, Jan 2017.
- [7] F. Alvarado, "The stability of power system markets," *IEEE Transactions on Power Systems*, vol. 14, no. 2, pp. 505–511, 1999.
- [8] M. Roozbehani, M. A. Dahleh, and S. K. Mitter, "Volatility of power grids under real-time pricing," *IEEE Transactions on Power Systems*, vol. 27, no. 4, pp. 1926–1940, 2012.
- [9] M. S. Nazir and I. A. Hiskens, "Load synchronization and sustained oscillations induced by transactive control," in *IEEE Power and Energy Society General Meeting*, 2017, pp. 1–5.
- [10] D. S. Callaway and I. A. Hiskens, "Achieving controllability of electric loads," *Proceedings of the IEEE*, vol. 99, no. 1, pp. 184–199, Jan 2011.
- [11] L. Zhao and W. Zhang, "Stability Analysis of Multi-Period Electricity Market with Heterogeneous Dynamic Assets," *arXiv preprint*, 2017. [Online]. Available: <http://arxiv.org/abs/1703.10267>
- [12] S. Koch, J. L. Mathieu, and D. S. Callaway, "Modeling and Control of Aggregated Heterogeneous Thermostatically Controlled Loads for Ancillary Services," in *Proceedings of the 17th Power Systems Computation Conference*, 2011.
- [13] J. L. Mathieu, S. Koch, and D. S. Callaway, "State estimation and control of electric loads to manage real-time energy imbalance," *IEEE Transactions on Power Systems*, vol. 28, no. 1, pp. 430–440, 2013.
- [14] L. C. Totu, R. Wisniewski, and J. Leth, "Demand response of a tcl population using switching-rate actuation," *IEEE Transactions on Control Systems Technology*, vol. 25, no. 5, pp. 1537–1551, Sept 2017.
- [15] M. S. Nazir, F. D. Galiana, and A. Prieur, "Unit Commitment Incorporating Histogram Control of Electric Loads With Energy Storage," *IEEE Transactions on Power Systems*, vol. 31, no. 4, pp. 2857–2866, 2016.
- [16] R. A. Verzijlbergh, L. J. De Vries, and Z. Lukszo, "Renewable Energy Sources and Responsive Demand. Do We Need Congestion Management in the Distribution Grid?" *IEEE Transactions on Power Systems*, vol. 29, no. 5, pp. 2119–2128, 2014.
- [17] A. Dubey and S. Santoso, "Electric Vehicle Charging on Residential Distribution Systems: Impacts and Mitigations," *IEEE Access*, vol. 3, pp. 1871–1893, 2015.
- [18] S. Hanif, T. Massier, H. Gooi, T. Hamacher, and T. Reindl, "Cost Optimal Integration of Flexible Buildings in Congested Distribution Grids," *IEEE Transactions on Power Systems*, vol. 32, no. 3, pp. 2254–2266, 2017.
- [19] S. Hanif, H. B. Gooi, T. Massier, T. Hamacher, and T. Reindl, "Distributed Congestion Management of Distribution Grids under Robust Flexible Buildings Operations," *IEEE Transactions on Power Systems*, vol. 32, no. 6, pp. 1–1, 2017.
- [20] M. D. Ilić, L. Xie, and J. Y. Joo, "Efficient Coordination of Wind Power and Price-Responsive Demand Part I: Theoretical Foundations," *IEEE Transactions on Power Systems*, vol. 26, no. 4, pp. 1875–1884, 2011.
- [21] J. Mathieu, M. Kamgarpour, J. Lygeros, G. Andersson, and D. Callaway, "Arbitraging intraday wholesale energy market prices with aggregations of thermostatic loads," *IEEE Transactions on Power Systems*, vol. 30, no. 2, pp. 763–772, March 2015.
- [22] H. Hao, B. M. Sanandaji, K. Poolla, and T. L. Vincent, "A generalized battery model of a collection of Thermostatically Controlled Loads for providing ancillary service," *2013 51st Annual Allerton Conference on Communication, Control, and Computing, Allerton 2013*, 2013.
- [23] X. Zhou, E. Dall'Anese, L. Chen, and A. Simonetto, "An incentive-based online optimization framework for distribution grids," *IEEE Transactions on Automatic Control*, 2017.
- [24] A. C. Kizilkale and R. P. Malhame, "Collective target tracking mean field control for markovian jump-driven models of electric water heating loads," in *Proceedings of the IFAC World Congress*, 2014, pp. 1867–1872.
- [25] D. Docimo and H. Fathy, "Demand response using heterogeneous thermostatically controlled loads: Characterization of aggregate power dynamics," *Journal of Dynamic Systems, Measurement and Control*, vol. 139, no. 10, pp. 1–9, 2017.
- [26] M. S. Nazir and I. A. Hiskens, "Noise and parameter heterogeneity in aggregate models of thermostatically controlled loads," in *Proceedings of the 20th IFAC World Congress*, 2017, pp. 8888–8894.
- [27] A. Pikovsky, M. Rosenblum, and J. Kurths, *Synchronization: A Universal Concept in Nonlinear Sciences*, 2003.
- [28] I. A. Hiskens and P. Bhaegerath, "Switching-induced stable limit cycles," *Nonlinear Dynamics*, pp. 575–585, 2007.
- [29] S. Bashash and H. K. Fathy, "Modeling and control insights into demand-side energy management through setpoint control of thermostatic loads," in *2011 American Control Conference*, 2011.
- [30] W. Zhang, J. Lian, C.-Y. Chang, and K. Kalsi, "Aggregated Modeling and Control of Air Conditioning Loads for Demand Response," *IEEE Transactions on Power Systems*, vol. 28, no. 4, pp. 4655–4664, 2013.
- [31] D. Paccagnan, M. Kamgarpour, and J. Lygeros, "On the Range of Feasible Power Trajectories for a Population of Thermostatically Controlled Loads," in *IEEE 54th Annual Conference on Decision and Control*, 2015.
- [32] M. Alizadeh, A. Scaglione, A. Applebaum, G. Kesidis, and K. Levitt, "Reduced-Order Load Models for Large Populations of Flexible Appliances," *IEEE Transactions on Power Systems*, vol. 30, no. 4, pp. 1758–1774, 2015.
- [33] K. X. Perez, W. J. Cole, J. D. Rhodes, A. Ondeck, M. Webber, M. Baldea, and T. F. Edgar, "Nonintrusive disaggregation of residential air-conditioning loads from sub-hourly smart meter data," *Energy and Buildings*, vol. 81, pp. 316–325, 2014.
- [34] "Ercot hourly load data," 2017. [Online]. Available: http://www.ercot.com/gridinfo/load/load{ }_hist/
- [35] S. Bashash and H. K. Fathy, "Modeling and control of aggregate air conditioning loads for robust renewable power management," *IEEE Transactions on Control Systems Technology*, vol. 21, no. 4, pp. 1318–1327, 2013.
- [36] J. Lofberg, "YALMIP : a toolbox for modeling and optimization in MATLAB," in *2004 IEEE International Conference on Robotics and Automation*, 2004, pp. 284–289.
- [37] R. Li, Q. Wu, and S. S. Oren, "Distribution locational marginal pricing for optimal electric vehicle charging management," *IEEE Transactions on Power Systems*, vol. 29, no. 1, 2014.
- [38] L. Bai, J. Wang, C. Wang, C. Chen, and F. F. Li, "Distribution Locational Marginal Pricing (DLMP) for Congestion Management and Voltage Support," *IEEE Transactions on Power Systems*, vol. 99, 2017.
- [39] R. Malhame and C.-Y. Chong, "Electric load model synthesis by diffusion approximation of a high-order hybrid-state stochastic system," *IEEE Transactions on Automatic Control*, vol. 30, no. 9, pp. 854–860, Sep 1985.
- [40] R. E. Mortensen and K. P. Haggerty, "Stochastic computer model for heating and cooling loads," *IEEE Transactions on Power Systems*, vol. 3, no. 3, pp. 1213–1219, 1988.
- [41] D. S. Callaway, "Tapping the energy storage potential in electric loads to deliver load following and regulation, with application to wind energy," *Energy Conversion and Management*, vol. 50, no. 5, pp. 1389–1400, 2009.



Md Salman Nazir (S10-M13) received his B.Eng. (Honours) and M.Eng. (Thesis) degrees, both in Electrical Engineering, from McGill University, Montreal, Canada in 2011 and 2015, respectively. He is currently pursuing his Ph.D. degree in Electrical and Computer Engineering at the University of Michigan, Ann Arbor, MI, USA. During 2012–2014, he was an engineer at the Natural Resources Canada's CanmetENERGY laboratory. His research interests include operations, control and economics of power systems in the presence of significant

renewable and distributed energy resources.



Ian A. Hiskens (F06) is currently the Vennema Professor of Engineering with the Department of Electrical Engineering and Computer Science, University of Michigan, Ann Arbor, MI, USA. He has held prior appointments in the Queensland electricity supply industry, and various universities in Australia and the United States. His research interests lie at the intersection of power system analysis and systems theory, with recent activity focused largely on integration of renewable generation and controllable loads. Dr. Hiskens is actively involved in various

IEEE societies and was VP-Finance of the IEEE Systems Council. He is a Fellow of IEEE, a Fellow of Engineers Australia and a Chartered Professional Engineer in Australia.